J. Phys.: Condens. Matter **21** (2009) 423101 (16pp) doi:10.1088/0953-8984/21/42/423101

TOPICAL REVIEW

Molecular dewetting on insulators

S A Burke[1], J M Topple[2] and P Grütter[2]

[1] Department of Physics, University of California Berkeley, Berkeley, CA, USA
[2] Department of Physics, McGill University, Montreal, QC, Canada

E-mail: saburke@berkeley.edu

Received 1 July 2009, in final form 4 August 2009
Published 8 September 2009
Online at stacks.iop.org/JPhysCM/21/423101

Abstract

Recent attention given to the growth and morphology of organic thin films with regard to organic electronics has led to the observation of dewetting (a transition from layer(s) to islands) of molecular deposits in many of these systems. Dewetting is a much studied phenomenon in the formation of polymer and liquid films, but its observation in thin films of the 'small' molecules typical of organic electronics requires additional consideration of the structure of the interface between the molecular film and the substrate. This review covers some key concepts related to dewetting and molecular film growth. In particular, the origins of different growth modes and the thickness dependent interactions which give rise to dewetting are discussed in terms of surface energies and the disjoining pressure. Characteristics of molecular systems which may lead to these conditions, including the formation of metastable interface structures and commensurate–incommensurate phase transitions, are also discussed. Brief descriptions of some experimental techniques which have been used to study molecular dewetting are given as well. Examples of molecule-on-insulator systems which undergo dewetting are described in some detail, specifically perylene derivatives on alkali halides, C_{60} on alkali halides, and the technologically important system of pentacene on SiO_2. These examples point to some possible predicting factors for the occurrence of dewetting, most importantly the formation of an interface layer which differs from the bulk crystal structure.

(Some figures in this article are in colour only in the electronic version)

Contents

1. Introduction

The production, characterization and growth of organic materials has received substantial attention in recent years, particularly with an eye towards use as functional components in devices [1, 2]. The potential for mass production of complex nanoscale objects with a wide range of engineered functionality through chemical means makes the use of organic materials extremely attractive. Indeed, the use of organic thin films in electronic and optoelectronic device applications has seen a great deal of progress to date with products already to market, and the promise of novel, inexpensive low energy processed devices ranging from flexible displays to low-cost, light-weight solar panels lingering on the horizon [3]. However, molecular materials are often sensitive to their local environment, and as such, the microscopic interfaces in any functional organic composite or device must be carefully understood and controlled. Despite the progress that has been

made in developing thin film organic materials for electronic applications, there remain fundamental questions regarding the influence of the device environment (i.e. electrodes, dielectric, encapsulation, and ambient conditions) on the properties of organic semiconductors. For example, while it is known that the molecule–dielectric interface and arrangement of molecules within the first few layers is critical to organic thin film transistor device performance [4–7], these systems have been particularly difficult to explore on the molecular/atomic scale due to a lack of suitable tools and complications in applying many well-established surface science techniques to both molecules and insulators.

One of the first steps in optimizing organic thin film devices then is to better understand molecular epitaxy and growth on substrates of interest. This includes metallic substrates which define the molecule–electrode interface, as well as insulating substrates which constitute the molecule–dielectic interface. There has been significant effort in studying organic film growth on a variety of substrates in recent years for this reason [1, 8, 9, 2]. In the study of the growth of thin and ultrathin organic films, the process of dewetting, whereby a film is broken up into crystallites or islands, has been observed on a number of substrates. Some examples where molecular dewetting has been observed include: pentacene on gold [10–12], 3,4,9,10-perylene tetracarboxylic dianhydride (PTCDA) on Ag(111) [13], perylene on Cu(110) and Au(111) [14], hexaazatriphenylene-hexacarbonitrile on Au [15], pentacene on SiO_2 [12, 16], phenylthiophene fulgide on quartz [17], m-bis(4-n-octyloxystyryl)-benzene on mica [18], diindenoperylene (DIP) on SiO_2 [19, 20], C_{60} on KBr and NaCl [21], PTCDA on NaCl [22] and KCl [23], 3,4,9,10-perylene tetracarboxylic diimide (PTCDI) on NaCl [24], and N,N'-dimethylperylene-2,4,9,10-bis(dicarboximide) (DiMe-PTCDI) on NaCl [25]. Dewetting relates to the issue of stability of films, and much like other roughening transitions, for organic thin film devices these changes in the large scale structure of the film, giving rise to holes and grain boundaries, may influence electronic and optoelectronic properties. Additionally, dewetting is often accompanied by a rearrangement of the interface layer and these differences in structure may alter the properties of the film near critical interfaces [26].

For device design and characterization, it is important to understand not just the structure and the resulting device-related properties, but also the long-term and thermal stability of the grown film. Organic films which undergo structural transition via annealing may then have limited range of acceptable processing temperatures and even operating temperatures. Similarly, if dewetting of an organic film occurs over a very long timescale, the device properties may change over time, likely a very undesirable effect. An understanding of *both* the structures formed during growth and the equilibrium morphologies and crystal structures are important to the successful development of technologies based on organic thin films.

This review will cover aspects of organic film growth and dewetting, in particular focusing on possible predicting factors for dewetting of organic thin films. From the list above, one can note that organic thin films on insulating substrates appear particularly susceptible to undergoing dewetting processes. Since dewetting appears to be particularly prevalent for molecules on insulators, which are integral to device applications such as OTFTs, the specific conditions of these systems which may lead to dewetting will be addressed. Several examples of organic thin films on insulating substrates are discussed in some detail, specifically perylene derivatives on alkali halides, C_{60} on alkali halides, and the technologically important system of pentacene on SiO_2, in order to illustrate some of the features of dewetting systems and to highlight where further understanding is needed. While the focus of this article will be primarily on insulating substrates, the features and origins of dewetting are expected to be shared by organic films on other substrates where this process occurs.

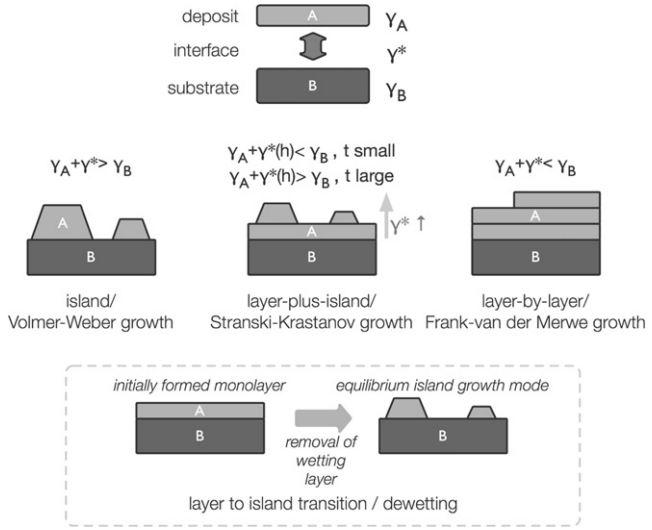

Figure 1. Schematic illustration of growth modes. The deposit (A) and substrate (B) each have surface energies γ_A and γ_B respectively, as well as an energy arising from the interface between the two, γ^*. The balance of these energies gives rise to different growth modes: island, Stranski–Krastanov, and layer-by-layer (middle, left to right). Another possibility is that the system forms closed layers which are not stable and a transition can occur resulting in islands formed from these initial layers, which is known as dewetting.

2. Surface energies, growth modes and dewetting

There are many treatments of the relation of surface energies to growth modes in the literature [27–30], however, the following will review some key concepts which are related to dewetting. The equilibrium growth of macroscopic films is dictated by the balance of surface energies of the substrate, γ_B, the deposit, γ_A and the energy of the interface, $\gamma*$ formed between the two (see figure 1), all of which are related to the change in Gibbs free energy required to create the surface or interface [27]. If the energies of the deposit surface and the interface are greater than the surface energy of the substrate, $\gamma_A + \gamma* > \gamma_B$, the interface and surface area of the deposit will be minimized and islands or crystallites will be formed in the so-called Volmer–Webber or island growth mode. While under real growth conditions these may eventually grow into a continuous film

as the space between islands is filled in, the film will show evidence of these origins in the form of grain boundaries and increased roughness. If instead, the balance of energies favours increasing the area of the deposit (and the interface) over leaving an exposed substrate surface, $\gamma_A + \gamma* < \gamma_B$, the film growth will proceed in a layer-by-layer fashion, also known as the Frank–van der Merwe growth mode. This will typically result in smooth films so long as diffusion is sufficient to permit completion of one layer before the nucleation of subsequent layers occurs. A third equilibrium growth mode occurs when the interface energy depends on thickness, for example when strain at the interface is gradually released in subsequent layers, resulting in a combination of layer growth followed by islands which nucleate on top of the initial 'wetting' layer. This layer-plus-island, or Stranski–Krastanov, growth mode is sometimes exploited in the fabrication of self-assembled nanoscale structures (for example, self-assembled quantum dot structures formed from semiconductor heterostructures). The prediction of growth mode in this way by the balance of surface energies is valid for the equilibrium case, however, growth is often not an equilibrium processes and kinetic parameters such as temperature, deposition rate and energy of the incident particles can also play a significant or even dominant role in determining growth morphologies.

In vacuum deposited films the 'dewetting' scenario arises when an initial film is formed during the non-equilibrium growth phase but is not the favoured morphology of the deposited film, or, when one form is favoured for a very thin film but cannot support the growth of a thicker film. Dewetting is a film evolution process by which islands or crystallites are formed through the removal of a pre-existing wetting layer. This is in contrast to the Stranski–Krastanov growth mode whereby the wetting layer remains and is typically stable, i.e. the islands formed do not grow through the removal of the wetting layer. The process of dewetting is well known with respect to the evolution of liquid and polymer films [31–35] and the evolution for crystalline films follows a similar progression: the film is broken up through the formation of holes and/or droplets leading to the final non-wetting state [36]. As this evolution takes place through a mass transport process from the wetting layer into 3D crystallites or islands, dewetting can be categorized as a form of coarsening or ripening. As in Ostwald ripening, where large droplets are more stable and grow at the expense of small droplets, dewetting proceeds as a competitive process whereby more stable features grow at the expense of a less stable population. If the wetting layer is sufficiently stable, or if diffusion barriers are high and effectively trap the wetting layer, annealing may be necessary to initiate and/or accelerate the process.

The conditions for dewetting are similar in terms of surface energy to Stranski–Krastanov growth: the free energy, F, must have a dependence on the thickness of the film, e. This typically occurs for thin films when the thickness of the film becomes of order the range of the interaction of the deposited layer with the substrate. This can arise as a result of van der Waals interactions, electrostatic interactions, or other long range interactions, which can include those related to structuring of the liquid, polymer or crystalline deposit [30, 29, 37]. These interactions give rise to a correction term, $P(e)$ in the free energy of the deposited film which is thickness dependent:

$$\frac{\mathrm{d}F\,(e)}{\mathrm{d}A} = \gamma^* + \gamma_A + P(e) \tag{1}$$

or in terms of the surface tension of the film:

$$\gamma_{A,\mathrm{film}} = \gamma^* + \gamma_A + P(e) + e\Pi(e) \tag{2}$$

where we have defined what is known as the 'disjoining pressure' as $\Pi = \partial P/\partial e$ [30]. Note that often the disjoining pressure is stated as $\Pi = \partial F/\partial e$, which is equivalent since the surface energies of the two solids are independent of the thickness (this is encapsulated in the correction term $P(e)$).

The stability of wetting films are often characterized in terms of the disjoining pressure which represents the difference between intermolecular interactions within the bulk and those within an adsorbed film interacting with the substrate. If the film is unstable ($P''(e) < 0$), the film will undergo spontaneous dewetting and fluctuations in temperature and density can be amplified in the so-called 'spinodal' regime [38], potentially giving rise to interesting morphological features. If the film is instead metastable ($P''(e) > 0$), the film dewets through the nucleation and expansion of denuded zones [30]. The dependence of the disjoining pressure on film thickness can be complex depending on the types and ranges of interactions involved and whether structuring of the film near the surface contributes an additional significant term and/or results in the existence of multiple isotherms [37]. This might include the presence of different structures in a thin and a thick film. Measurement of the disjoining pressure as a function of thickness has also been used to describe the evolution of the film morphology from film growth through nucleation of droplets, holes and finally holes induced by substrate defects [33].

The form of this correction term, and therefore the disjoining pressure, depends on the specific interactions involved in the system to be considered. For example, when van der Waals interactions dominate, which is the most commonly considered case, this term can be written as:

$$P(e) = \frac{A}{12\pi e^2} \tag{3}$$

where A is the Hamaker constant. However, for ultrathin films, where the thickness approaches the atomic or molecular dimensions of the deposit, modelling of the specific system to be described is required as the structure of the film and the interplay of different interactions play a significant role [30].

Nevertheless, the concept of disjoining pressure may also be useful in the description of dewetting of crystalline molecular films. Here, the disjoining pressure arises from the competition between intermolecular and adsorption (molecule–substrate) forces, much as in the case of liquid and polymer films. The crystalline structure can give rise to interface structures that differ significantly from the bulk structure either due to an imposed commensurability from the substrate [22], or an adsorption geometry which differs

from the bulk structure, for example a different tilt angle of molecules at the surface [6]. These interface structures may be incompatible with the bulk structure leading to strain, or in more extreme cases a forced rearrangement of the interface, giving rise to thickness dependent interactions.

For illustration purposes, we can consider a simplified 1D case of an imposed commensurability with the substrate lattice. No problem arises in the case where the deposited molecular lattice and the substrate lattice match, or nearly match, in both lattice constant and geometry (see figure 2(a)). However this is often not the case for molecules deposited on inorganic crystalline substrates [39]. If the intermolecular binding energy is of the same order as the adsorption energy, but the lattices are mismatched, the situation where there are two nearly equal energy adsorption sites can occur (see figure 2(b)): one which is commensurate with the substrate lattice (metastable) and one which is close to the bulk lattice constant of the molecular material (stable). Depending on the precise energy balance and the size of the barrier formed between the two states in comparison to the thermal energy, a metastable commensurate phase may form and even be stable at a given temperature. The formation of these different possible epitaxies as a result of lattice geometry and competing interactions can set up the conditions for dewetting. In the metastable commensurate state the molecule–substrate interaction dominates and we expect wetting of this phase, but not necessarily of the bulk-like phase where intermolecular interactions dominate. In terms of the free energy and the disjoining pressure, this amounts to different paths, or isotherms, of the free energy with respect to thickness of the film due to each distinct structure. In these cases the dewetting transition is also accompanied by a change of the interface structure from commensurate to incommensurate. This accompanying commensurate–incommensurate transition may further assist the dewetting process by providing dislocations [40] for hole formation to begin. While this is a simplified model to illustrate the possibility of a metastable state which could give rise to dewetting, real molecular systems have additional factors which should be considered, including additional degrees of freedom such as rotation and conformation, anisotropic interactions between molecules and between the molecule and substrate, and relatively soft interactions allowing for greater strain in molecular lattices. This can give rise to substrate imposed geometries of the molecular lattice which are quite different from the bulk, for example the formation of a brickwall structure in PTCDA as opposed to the usual herringbone lattice found in the bulk [23], as well as the more common occurrence of multiple epitaxies which have similar energies. Specific examples of these transitions for crystalline organic films on alkali halides are given in section 4, followed by the technologically important system of pentacene on silicon oxide which exhibits a dewetting transition which may be accompanied by a change in molecular orientation as well as lattice parameters.

It is important to note that molecular epitaxy and growth bears some significant distinctions from inorganic crystal growth. For a detailed examination see recent reviews by Hooks *et al* [39], Witte and Wöll [8], and Kowarik *et al* [41].

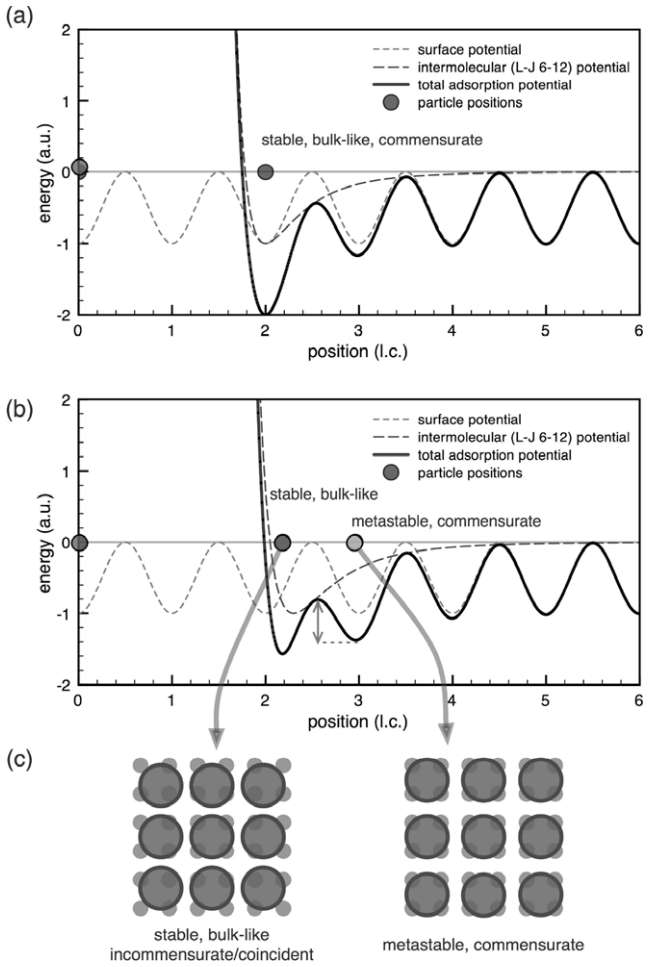

Figure 2. Competition of intermolecular and adsorption potentials for a commensurate deposit (a) and an incommensurate deposit (b). In the latter case, a nearly commensurate metastable adsorption site can appear which would give rise to the situation shown on the right in (c), despite the global minimum which is closer to the bulk molecular structure, but incommensurate shown on the left. A barrier is formed between the two which depends on the relative potential depths, degree of mismatch and precise form of the potentials.

In particular, intermolecular interactions and often molecular adsorption interactions are heavily dominated by van der Waals and electrostatic interactions. The predominance of these physisorption interactions combined with the large size of molecules compared to most inorganic unit cells often leads to total adsorption energies in the eV range, but with shallow walled potentials. The resulting soft interactions between molecules and between molecule and substrate leads to the ability of many organic materials to accommodate much larger strain than that allowed by most inorganic deposits [41]. This also gives rise to the common occurrence of polymorphs and multiple epitaxies since the presence of many similar minima arises more often in this situation. Coincident epitaxies are also more common in molecular deposits than in inorganic materials due to the softer interactions involved as well as the usually significant mismatch in unit cell size and geometry between molecular overlayers and inorganic substrate surfaces [39]. Molecules are also extended objects which have a number of extra degrees of freedom compared

to inorganic materials. Most importantly for growth and epitaxy, there are orientational degrees of freedom: which way are molecules oriented with respect to the substrate and to each other? This can give rise to different epitaxial patterns, for example brickwall versus herringbone arrangements of PTCDA [42, 23], or different tilt angles with respect to the substrate, for example pentacene [6]. Since this may enhance or restrict intermolecular interactions, the properties of the film may be influenced by these different orientational arrangements. Molecules also have conformational degrees of freedom, meaning that individual molecules can distort, for example to accommodate stress. The distortion of the conjugated backbone of a molecular semiconductor may shift energy levels [43–45] and therefore also influence film properties. These additional degrees of freedom and accommodation of strain can give rise to complex energy landscapes, and ones which may even change with the addition of subsequent layers due to the strength of intermolecular interactions compared to the molecule–substrate interaction.

Taking that crystalline molecular films can experience thickness dependent interactions giving rise to a change in the free energy with thickness, we now look to the relative surface energies of some typical substrates and organic materials. If the surface energies of the deposited material and the substrate are similar, the interface energy and any thickness dependant component will have a greater influence on the growth mode exhibited. Similarly, if the interface energy is very large, or the thickness dependent component is very large, it may dominate the growth. The values of some surface energies for some molecules, insulators and metals which may be of interest for experimental prototype samples or in technological systems are listed in table 1. Of particular note, is that the surface energies of some highly conjugated molecular materials are quite small compared to many metals, indicating that layer-by-layer growth should usually be preferable for these interfaces unless the interface energy is large enough to overcome the difference between the bulk surface energies. However, the surface energies of molecules and many insulators may be of similar magnitude leading to the situation where we expect the interface energy and any thickness dependent component of the free energy to have a significant effect on the resulting growth mode. In this case, the effects described above, specifically the potential for multiple epitaxies, commensurate–incommensurate transitions, possible changes in molecular orientation and ordering with increasing thickness, can lead to the conditions for dewetting. In these systems where there is close competition between the bulk surface energies, we should look to the details of the interface to find whether we expect dewetting phenomena.

Table 1. Surface energies of some organic crystals, insulators and metals for comparison.

	Material	Surface energy (J m^{-2})
Molecules	C_{60}	0.116 [46]
	Pentacene	0.0496 [47]
	Anthracene	0.0528 [47]
Insulators	KBr(100)	0.151 [48]
	NaCl(100)	0.188 [48]
	LiF(100)	0.169 [48]
	SiO_2	0.05–0.06 [49, 50]
Metals	Au	1.333 [51]
	Pd(111)	1.64–2.00 [52]
	Ta	2.493 [51]

3. Experimental methods for studying dewetting

A number of different surface characterization methods have been used to study dewetting. The key components of most dewetting studies include: (1) measurement of the coverage of the surface, (2) a characterization of the epitaxy, interface structure and/or film structure, and (3) a characterization of the resulting film morphology. While many techniques used to study growth provide this type of information, often a combination of measurement techniques has been used. Very often *in situ* high vacuum (HV) or ultrahigh vacuum conditions (UHV) are used to ensure cleanliness of the substrate surface and deposit material since impurities may influence both growth and dewetting behaviour and are difficult to characterize and describe. Below, a few of the key techniques appearing in recent molecular dewetting studies are briefly described.

Scanning probe microscopies (SPM) can provide a powerful real space visualization of both the molecular scale structure and the morphologies present at various stages of growth. Scanning tunnelling microscopy (STM), which uses tunnelling current for tip–sample distance regulation, has been used extensively for investigations of molecular growth on conducting surfaces [53, 42, 54–58] or thin insulating films [59, 60]. However, on thick or bulk insulators STM cannot be used, and often molecular films require the use of very small tunnelling currents [42] due to their lower conductivity which puts these materials out of reach for many instruments. The technique of non-contact atomic force microscopy (nc-AFM) does not require the use of a conducting substrate and in many cases can provide the molecular and atomic resolution required to elucidate the structure and epitaxy of molecular deposits [61–64, 22, 23, 65]. These high resolution studies are performed in UHV by nc-AFM, or frequency modulation AFM, which makes use of the frequency shift induced in an oscillating cantilever by the tip–sample interaction [66]. Other AFM techniques can also provide important information about film morphology.

While individual SPM techniques may have particular advantages or drawbacks, the key disadvantage with using these for the study of growth is their snap-shot nature. Due to the time required to acquire STM or AFM images and the localized nature of the measurement it is difficult to capture dynamics of the system unless they occur over a timescale that is slow enough to be sampled at a reasonable rate but not so slow that cleanliness of the sample cannot be maintained. Additionally, one must take care to ensure that the presence of the tip does not influence the molecular deposits, especially where relatively unstable or metastable structures are investigated.

Photoemission spectroscopy, while usually used to characterize electronic structure and chemical composition,

has been used to dynamically monitor coverage for dewetting studies [10, 14, 15, 12]. Photoemission spectroscopy is performed by illuminating the sample with light (ultraviolet for UPS or x-rays for XPS) and measuring the intensity of energy resolved electrons emitted. The kinetic energy of the emitted electrons is related to the density of states. UPS is sensitive to valence band states and is generally used to measure band structure and surface states. XPS excites core holes which provide chemical information about the sample. Since XPS is not especially surface sensitive, grazing incidence is sometimes used to probe only surface features [28].

In dewetting studies, XPS signals corresponding to the substrate composition and the deposit composition are used to determine the relative areas of the exposed substrate surface and deposit covered area by monitoring a chemical signature of either the deposited material, the substrate surface or both. This can be done as a function of time, annealing temperature, or during deposition. The interpretation of XPS data for determining the covered area of the substrate requires the development of a 3d growth model such as that used by Käfer *et al* [12]. However, a benefit of this technique is the ability to monitor the growth during and post-deposition *in situ*.

Techniques which can determine film structure, especially at or near the interface are also important for the study of dewetting mechanisms. Near-edge x-ray absorption fine structure (NEXAFS) provides a complimentary technique that is sensitive to molecular orientation, which can be an important factor in dewetting [10, 11]. X-ray diffraction (XRD) has also been used to study the film structure which is then related to dewetting [13, 11, 12, 15]. Since the final morphology may be strongly influenced by the dewetting process, *ex situ* characterization by optical microscopy, scanning electron microscopy (SEM) and AFM have also been applied.

It should be noted that care must be taken when investigating organic materials with x-ray and electron based measurements to ensure that the beam does not induce changes in the materials probed. Additionally, when insulating materials are used, damage or charging of the substrate may create further complications. While each of these techniques has individual strengths, ideally a combination of measurements to characterize both dynamics and structure would be applied *in situ* to fully capture the dewetting process, the resulting morphology and the driving forces behind the transition.

4. Examples of molecule-on-insulator growth exhibiting dewetting

4.1. Perylene derivatives on alkali halides: epitaxy driven dewetting

Perylene derivatives constitute a group of molecules which consist of a perylene core (a rectangular arrangement of 5 six carbon rings) but can have a variety of different attached functional groups (see figure 3 for examples discussed herein). The perylene core is aromatic and most perylene derivatives are highly conjugated, or have a highly conjugated region. The most common perylene derivatives are based on

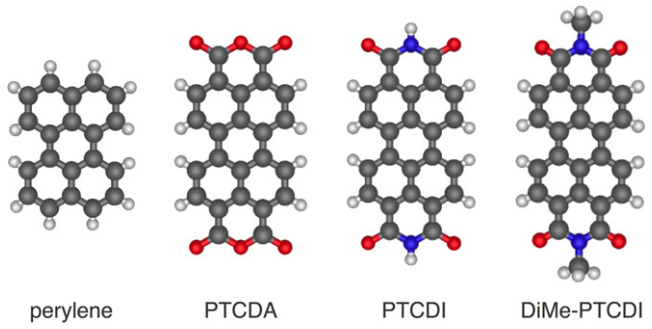

Figure 3. Perylene derivatives discussed, from left to right: perylene, PTCDA, PTCDI, and DiMe-PTCDI.

3,4,9,10-perylene tetracarboxylic diimide (PTCDI) which can be synthesized with a variety of different groups attached to the nitrogen atom contained in the imide groups at either end of the molecule. Another commonly studied, commercially available, perylene derivative is the red dye 3,4,9,10-perylene tetracarboxylic dianhydride (PTCDA) which has three oxygen atoms at each end of the perylene core. Both PTCDA and PTCDI have partial charge separation within the molecule giving rise to a quadrupole moment where the oxygen atoms have a negative partial charge and the hydrogen terminated edges of the molecules have a partial positive charge.

The growth of 3,4,9,10-perylene tetracarboxylic dianhydride (PTCDA) has been studied on many surfaces [8, 13, 42, 67–69, 23, 22, 70, 53]. This planar conjugated molecule typically adsorbs parallel to the surface, and in the bulk arranges in a herringbone lattice with a small shift between layers in two different crystallographic directions giving rise to the α and β polymorphs [71]. A type of dewetting transition was observed for PTCDA on Ag(111) [13] which changes from layer-by-layer growth to layer-plus-island or Stranski–Krastanov due to a chemisorbed first layer. As one of several prototypical organic semiconductors the modes of PTCDA film growth are of some interest, perhaps especially on dielectric surfaces. The growth of low coverages of PTCDA on alkali halides has recently gained some attention and PTCDA on NaCl [22] and KBr have been studied by nc-AFM, and PTCDA on KCl has been studied by both nc-AFM and differential reflectance spectroscopy (DRS) [23].

Submonolayer coverages of PTCDA on NaCl [22] exhibit predominantly monolayer islands with a basketweave $p3 \times 3$ commensurate lattice resulting from the interaction between the partially negatively charged oxygen atoms at the ends of the molecule with the Na^+ ions of the substrate surface. As a complete layer is approached at $\sim$0.85 ML a coexistence between monolayer islands and multilayer ($>$3 layers) crystallites was observed, similar to the bimodal growth reported for the inorganic system Au on $SrTiO_3$ [72]. These newly formed multilayer crystallites appear to have a herringbone lattice, the bulk-like structure, and usually have a region of bare substrate surrounding these islands indicating that the material now contained in the crystallite originated in the monolayer film (see figure 4(c)). This dewetting transition, which is triggered by increasing coverage, is a result of the competition between the substrate interaction

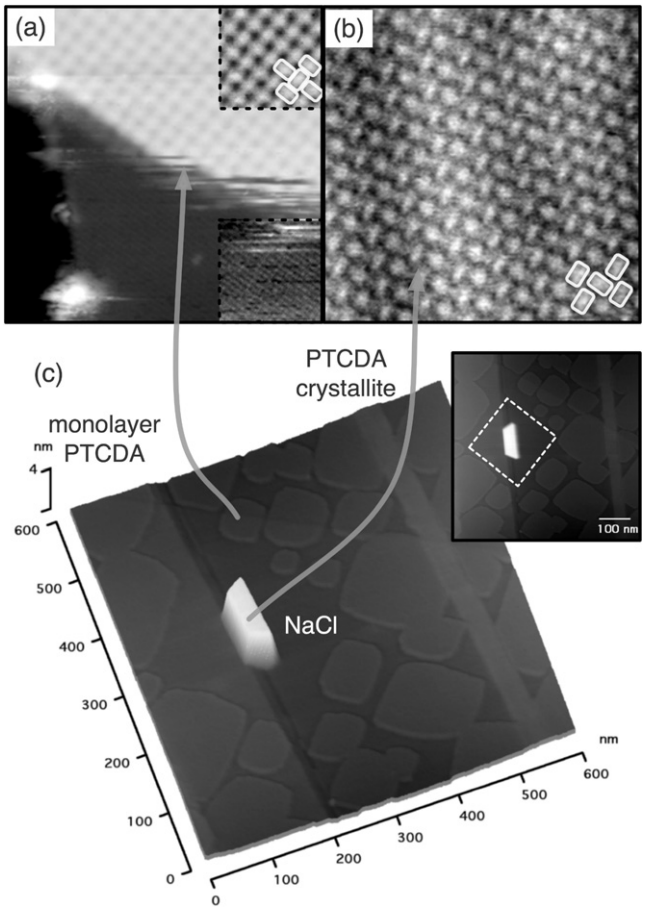

Figure 4. nc-AFM images of PTCDA on NaCl. (a) Commensurate $p3 \times 3$ monolayer structure, (b) herringbone arrangement of crystallites, and (c) overview showing coexistence of monolayer islands with crystalline island surrounded by bare NaCl surface [22].

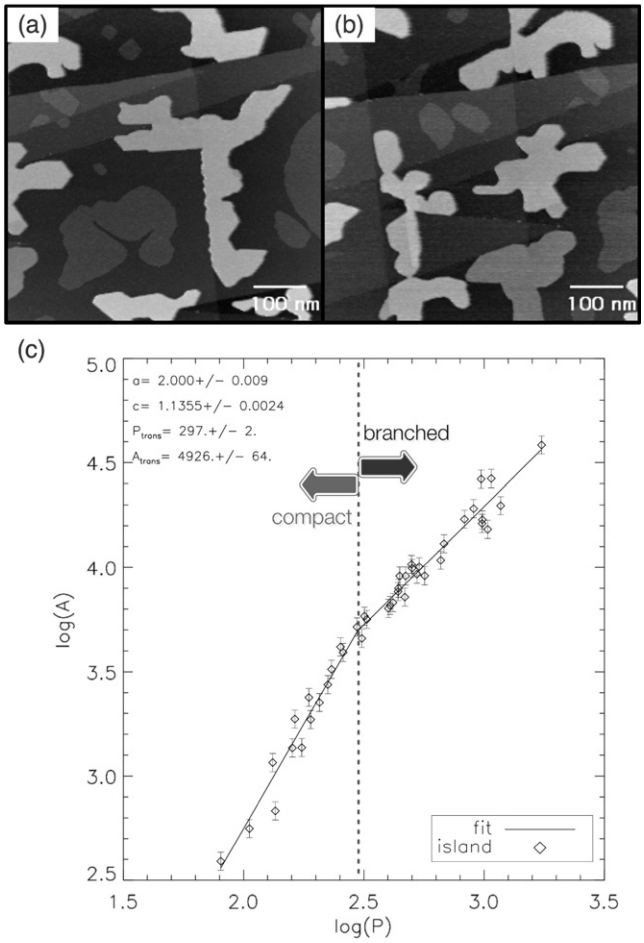

Figure 5. Larger coverages of PTCDA on NaCl (2ML shown here) also show a coexistence between ML islands and multilayer crystallites. (a), (b) show nc-AFM topography images of 2ML PTCDA on NaCl, (c) shows the perimeter–area relation plot for this coverage. Beyond a critical size, multilayer islands exhibit dendritic-like structures (branched), likely due to the haphazard addition of molecules through the continued dewetting of ML islands formed nearby [73].

favoured commensurate epitaxy and the bulk-like herringbone structure needed for the growth of subsequent layers. Since the monolayer structure differs too much from the bulk it cannot support the formation of additional layers. As the coverage is increased and additional layers must form, the structure at the PTCDA–NaCl interface is expected to adapt to an epitaxy more similar to the bulk. This change in the interface structure is accompanied by changes in both the interface energy and the surface energy of the molecular crystal leading to the observed dewetting transition rather than continued layer-by-layer growth.

As the coverage is increased further the coexistence between the two types of islands continues (see figures 5(a) and (b)). The bare substrate revealed by the dewetting process allows monolayer islands to continue to form. Multilayer crystallites continue to grow through addition of molecules in a normal growth process, but also likely through the continued dewetting of nearby monolayer islands as new critical coverages are achieved locally leading to growth by haphazard addition and the formation of non-compact island shapes (see figure 5(c)).

Regions of the substrate surface which have higher step density often show multilayer crystallites with a surrounding depletion of the monolayer islands at coverages well below the dewetting transition. The origins of this localized substrate structure induced dewetting are unclear at this point and could be a result of the local curvature [74] or due to nucleation of the crystallite phase at the step edge. While this presents an additional parameter which must be carefully controlled, the influence of substrate structures on the dewetting process points to a method of favouring the crystallite phase over the monolayer phase if so desired by tuning the substrate structure. Indeed, the use of charge induced desorption pits in NaCl does result in a dewetting transition occurring at a lower coverage though other structures are also observed [26].

Dewetting of the monolayer structure was also achieved by annealing. None of the monolayer islands were observed after annealing, indicating that this structure is metastable and is formed as a result of kinetics during growth. Annealing gives the system sufficient energy to rearrange by diffusion, as well as overcome the barrier between the metastable monolayer and the stable bulk-like structure.

PTCDA on KCl, investigated by Dienel *et al* [23], exhibits a similar behaviour with a brickwall monolayer 2×2 commensurate phase at low coverages and a transition to bulk-like multilayer islands at higher coverages. At coverages of less than one monolayer, DRS measurements exhibit an anomalously sharp peak at a wavelength corresponding to monomer absorption. The commensurate brickwall epitaxy determined by nc-AFM measurements results in reduced intermolecular interactions, and the identical adsorption sites of this structure results in a narrower peak than that observed for less homogeneous environments, for example in chloroform solution or on mica. As the coverage is increased beyond a monolayer, the DRS spectrum evolves with time and after ∼1 h the DRS spectrum corresponds to that of thick polycrystalline PTCDA films. The nc-AFM observations reported correspond to the optical measurements showing stable monolayer islands with a brickwall structure at low coverage and multilayer islands with no monolayer between for coverages above 1 ML. This similar commensurate to incommensurate epitaxial transition accompanied by dewetting indicates that the balance of surface and interface energies of the two materials is strongly dependent on the interface, which for molecular materials can very often have multiple configurations.

In contrast to the growth of PTCDA on NaCl and KCl, on KBr no monolayer phase was observed at room temperature [75, 73]. While there is some evidence of strain at the interface as islands of less than 3 layers are not observed [64], the proposed $p2 \times 3$ epitaxy is both commensurate and close to the bulk lattice constants of PTCDA. This situation more closely resembles that of figure 2(a) and dewetting is not expected, i.e. one growth mode, in this case island growth, is expected. It is however possible that under different growth conditions other phases may form, but these would be expected to be less stable than the monolayer phases described above.

Similarly, DiMe-PTCDI, which was also studied by nc-AFM on alkali halides [25], is expected to form a commensurate structure (a $p2 \times 2$ brickwall structure) on KBr where no monolayers are observed, but on NaCl a nearly commensurate lattice was found for islands. An unstable monolayer was observed between multilayer islands at higher coverages on NaCl which dewets within several minutes of imaging the region with the material from this monolayer seen to add to the nearby stable multilayer islands.

The post-growth evolution of PTCDA and C_4-PTCDI films on alkali halides was observed several years earlier by Schlettwein *et al* [69]. In that study, *in situ* luminescence spectra indicated a temporal evolution of these perylene derivative films from monomer signatures to excimer, or bulk-like, signatures. In particular, PTCDA on KCl exhibited a strong, narrow monomer signature immediately after deposition of 1 ML or more which quickly decreased, shifting towards the excimer signature at longer wavelengths which corresponds well with the recent data of Dienel *et al* [23]. PTCDA on NaCl exhibited similar though less striking behaviour. While the corresponding high resolution structural data was not available for comparison, it is likely that the monomer signature arises from a commensurate monolayer structure which diminishes intermolecular interactions. *Ex situ* AFM measurements were performed to investigate island morphology, revealing interesting branched structures that dominate for PTCDA on NaCl and KCl surfaces. The island morphologies found for PTCDA on KBr appeared less branched, and more similar to that expected for PTCDA herringbone crystallites. Also studied, C_4-PTCDI on NaCl did not show any monomer signature at multilayer coverages, perhaps indicating that no weakly interacting monolayer structure is formed, while on KCl a similar strong, sharp monomer signature was observed in coexistence with the excimer signature even at coverages beyond 1 ML, perhaps indicating a Stranski–Krastanov type growth where the wetting layer remains.

Another perylene derivative, 3,4,9,10-perylene tetracarboxylic diimide (PTCDI), has also been studied by nc-AFM on NaCl [24]. PTCDI, which has nitrogen containing imide end groups instead of all oxygen, exhibits a different crystal structure in the bulk than PTCDA. Hydrogen bonding between the nitrogen and hydrogen atoms of the imide groups of adjacent molecules results in rows of molecules which are canted with respect to the row direction [76, 77, 56]. Since the charge distribution of the molecule is similar, PTCDI is expected to optimally adsorb with the imide groups at the ends of the molecule positioned over positive ions of an alkali halide substrate as observed for PTCDA.

Submonolayer coverages of PTCDI on NaCl show similar growth characteristics to PTCDA [24]. Square monolayer or bilayer islands are observed which have a commensurate 2×2 brickwall epitaxy. This is similar to the bulk in that the molecules are aligned end-to-end, but exhibits a distorted lattice and no obvious canting of the molecules with respect to the row direction. During or shortly after deposition, multilayer needle shaped crystallites begin to form and grow depleting the surrounding square islands (see figures 6(a)–(d)). As in the case of PTCDA, these needle shaped crystallites have a bulk-like structure with PTCDI molecules arranged end to end in canted rows and lattice constants similar to the bulk.

The dewetting transition for PTCDI on NaCl occurs over the course of several days at room temperature allowing for the observation of the evolution of both island populations. These were characterized from nc-AFM images taken through the progression of the dewetting process and empirically fit to a growth model given by:

$$\frac{\mathrm{d}P}{\mathrm{d}t} = \frac{1}{\tau}(P_\infty - P) \tag{4}$$

where P is the current population of molecules (size of the island), τ is a time constant $\tau > 0$, and P_∞ is the final population of molecules in the island. This gives the needle/bulk-like island population evolution as a function of time:

$$P = P_\infty - \delta \mathrm{e}^{-\frac{t}{\tau}} \tag{5}$$

where δ is the difference between the initial and final populations $(P_\infty - P_0)$. An analogous decay function was fit to the decreasing square island population:

$$P = P_0 \mathrm{e}^{-\frac{t}{\tau}}. \tag{6}$$

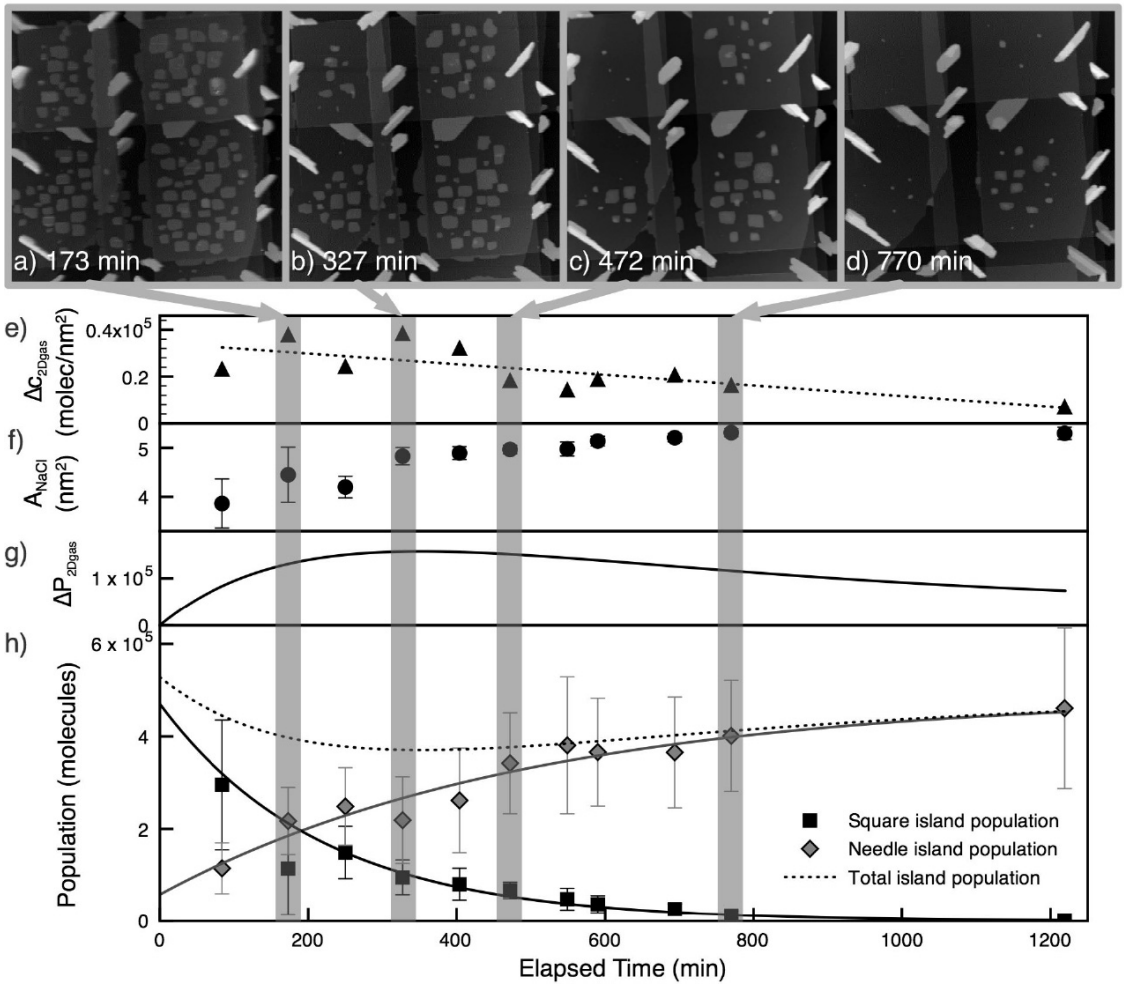

Figure 6. Sequence of nc-AFM images showing PTCDI dewetting on NaCl (a)–(d) with the change in the background concentration (e), the change in exposed NaCl area (f), the change in population of the PTCDI 2D gas (g), and the populations of each island type as a function of time (h). Reprinted with permission from [24]. Copyright (2009) by the American Physical Society.

Interestingly, the apparent total population of molecules found in the two island types is not constant with time. Rather this total population initially decreases and slowly recovers at long times. The 'missing' population is presumed to be in the form of a 2D gas diffusing over the surface, and provides the background concentration field through which the mass transport process of dewetting occurs. Due to the limited growth resources constrained by the initial deposition coverage, the concentration which feeds the growth of the needle islands is not constant with time, but steadily decreases until the square island population is entirely consumed. The rate equation for the 'monomolecular growth model' given above assumes that the growth rate of a particle (island) is proportional to the difference between the current and final size which is consistent with a finite number of units (molecules) in the system. As the particle size increases, the growth rate slows due to the reduction in available resources from the background concentration field [24].

Since the number of particles is fixed by the deposition amount, this form of the dynamics of island population is expected to be rather general. However, the rates of each process involved: dissolution of metastable islands and growth of stable islands, will depend on a number of system specific parameters. These include the stability of the metastable phase which relates to the net flux of molecules away from this phase, diffusion of molecules over the surface including across barriers such as steps, nucleation rates of the stable phase, and attachment rates to the stable phase which may be anisotropic. The complexity of the interplay of these molecular processes and their individual dependence on the atomic scale details (i.e. crystal structure and diffusion mechanisms) requires and deserves detailed theoretical attention. Ideally, multiscale methods (for example those used in [78, 79]) which can incorporate dynamics on different length and timescales would be applied to give a better understanding of how these different aspects influence the stability and final morphology of films which undergo dewetting.

These examples of dewetting of perylene derivatives on alkali halides highlight how the competition between commensurate and bulk structures can lead to dewetting. In these cases, the strain induced by the formation of a commensurate epitaxy which wets the surface leads to a rearrangement of the molecule–substrate interface upon further deposition, with annealing, or even with time. This lateral

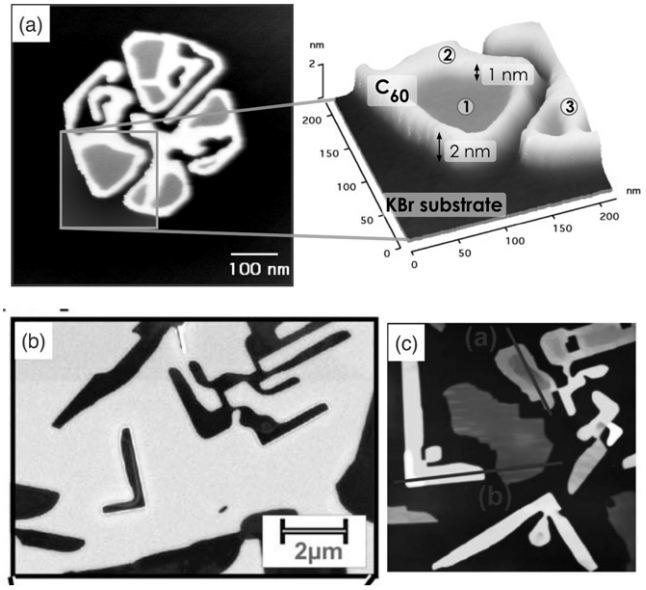

Figure 7. (a) Nc-AFM image of a C_{60} island on KBr with branched morphology exhibiting disconnected regions, enclosed monolayer areas and wrapped branches [21]. (b) SEM and (c) AFM of perylene on Cu(110) showing the similar 'skeleton' morphology as a result of dewetting [14]. (b) and (c) reprinted with permission from [14]. Copyright (2006) by Springer Science + Business Media.

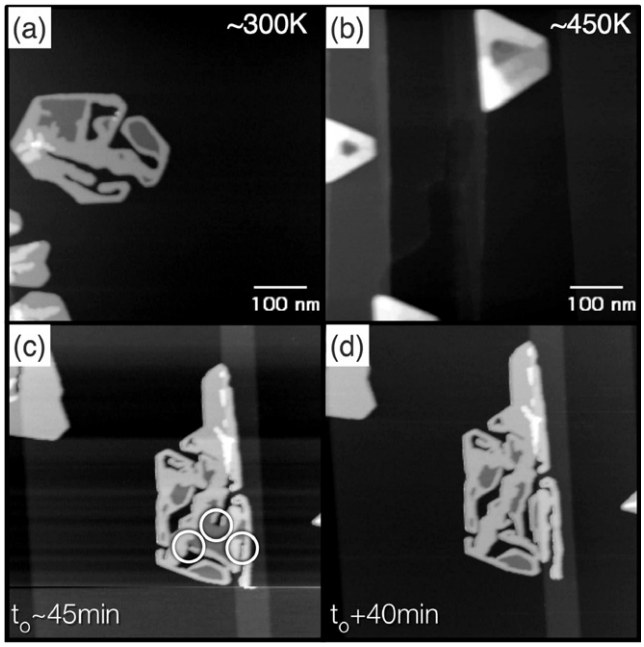

Figure 8. Nc-AFM image of C_{60} on KBr growth at room temperature (a) and ~450 K (b) under otherwise similar growth conditions (same rate and coverage). (c) and (d) show the final stages of spontaneous dewetting of C_{60} on NaCl, with (d) acquired 40 min after (c) in the same location. Circles in (c) indicate areas where 1st layer is exposed [21].

strain, which propagates with thickness, can also be considered as a structural component of the disjoining pressure which leads to dewetting. In describing the dynamics of PTCDI on NaCl dewetting a monomolecular growth model and analogous decay function was used to empirically fit the island populations as a function of time [24]. Also, perhaps important for the description of molecular dewetting dynamics, is that the background concentration field is not constant with time but decreases as the finite number of particles are consumed by the stable island population.

4.2. C_{60} on alkali halides: a morphological effect of dewetting

Growth of C_{60} fullerene molecules and fullerene derivatives in submonolayer coverages and thin films [80, 54, 55, 59, 81] has received considerable attention in recent years due to their interesting electronic and optoelectronic properties [82–84]. There have been several studies of C_{60} growth on alkali halides [80, 85–87] primarily with the aim of achieving large single crystal films on these weakly interacting substrates. At room temperature, submonolayer coverages of C_{60} on KBr and NaCl were found by nc-AFM to exhibit unique dendritic island shapes which appear to be a result of a dewetting process [62, 21].

The dendritic island shapes observed for C_{60} on KBr and NaCl have some unique features which are not generally observed for 'hit and stick' growth processes that result in dendritic island shapes [88]. The islands observed often exhibit branches which wrap back towards the centre of the island, and sometimes consist of several disconnected regions which have the same orientation and are localized in the same area (see figure 7(a)). Also, these islands consist of rims of two layers of C_{60} which often enclose single layer regions. However, single layer regions are not generally observed without this protecting rim structure [21].

Annealing to just below the evaporation temperature of the islands, or ageing of the samples for several days resulted in the disappearance of the enclosed monolayer regions. However, there was no overall rearrangement of the branched island shapes, likely due to significant C_{60}–C_{60} interactions and insufficient diffusion to 'heal' the island structures. In contrast, high temperature growth resulted in large, far-spaced islands with a compact triangular or elongated hexagonal shape (see figure 8) similar to that observed previously for high temperature growth [87], indicating that this is the equilibrium island shape.

Observations by nc-AFM of an island taken ~45 min after deposition at room temperature showed regions of monolayer C_{60} which was not enclosed due to a gap in the second layer rim (see figure 8(c)). Subsequent images show this monolayer film edge recede away from the gap and the formation of a bilayer rim structure and branches until the monolayer region was enclosed and consequently stabilized (see figure 8(d)). From these observations, it appears that the unusual shapes found for C_{60} islands on KBr and NaCl are formed as a result of a spontaneous dewetting process. The disconnected regions and internally pointing branches are formed by the 'ungrowth' of an unstable monolayer which is suspected to be formed during growth.

The general form of the branched islands observed for C_{60} on KBr and NaCl exhibits similarities to the 'skeleton' island structures described by Witte *et al* for perylene on

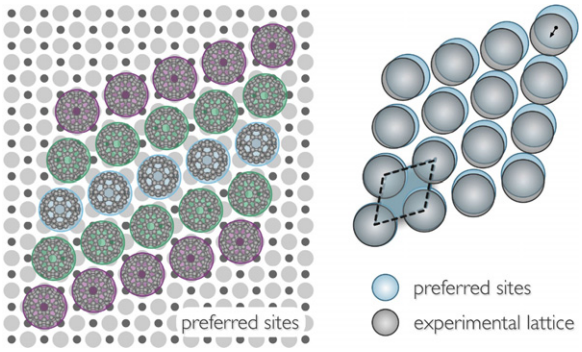

Figure 9. Preferred lattice sites for C_{60} on KBr determined from calculations (left) [90, 91, 45] and comparison with measured experimental lattice showing small contraction of lattice from this ideal adsorption epitaxy.

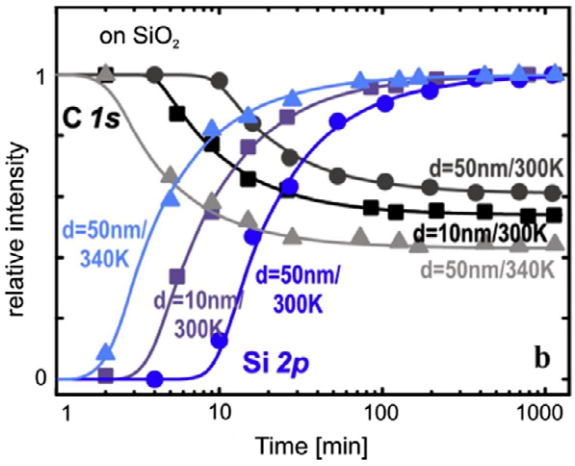

Figure 10. XPS intensity as a function of time after deposition for different film thickness and substrate temperatures. Reprinted with permission from [12]. Copyright (2009) by Springer Science + Business Media.

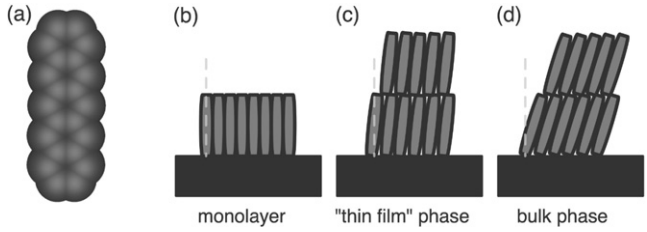

Figure 11. (a) Spacefill model of pentacene (hydrogen atoms not shown), (b)–(d) schematic representation of monolayer, thin film phase and bulk phase orientation of molecules with respect to the substrate (based on [6, 97]).

Cu(110) which were also formed by dewetting (see figures 7(b) and (c)) [14]. In particular, the appearance of rimmed structures with wide branches and holes which maintain the symmetry of the molecular crystal is consistent with the appearance of branched C_{60} islands. While for the case of perylene on Cu(110), dewetting is induced by annealing, for C_{60} on KBr and NaCl the process occurs spontaneously following growth [21], presumably due to the kinetic trapping of a monolayer structure during deposition similar to the case of PTCDI on NaCl [24] discussed above but on a faster timescale.

Phase field modelling of the C_{60} growth on alkali halides [89] was used to investigate island shape formation. A free energy consisting of a triple well representing the bare substrate, a metastable monolayer and a stable second layer was used. Given the correct parameters, a 'growth' period resulted in hexagonal monolayer islands which during an 'evolution' period were shown to evolve into islands with bilayer rims and interior monolayers or bilayer regions with interior holes. A variety of branched and disconnected structures could also be achieved by initiating the evolution period with notches or fluctuations in the edge density. The rather striking reproduction of the island shapes indicates that the formation of the branched island structures is a result of a dewetting process and that the variety of shapes are formed as a result of random variations in the initial shape of the monolayer island and/or fluctuations in the edges when dewetting begins.

Considering the molecular epitaxy once more, the observed bilayer and trapped monolayers were found to have a large coincident unit cell containing 142 molecules on KBr. Since the initial monolayer was not stable, the epitaxy for this state was not observed. However, comparing to calculated adsorption sites for C_{60} on KBr [91, 45], a similar, but commensurate lattice was found (see figure 9) [90]. The observed lattice is smaller than the lattice of favourable adsorption sites, and is closer to the C_{60}–C_{60} equilibrium distance [46]. Much like PTCDA, the commensurate lattice results in a strain in the molecular lattice that is likely allowable, however, intermolecular interactions appear to overcome the influence of the adsorption potential and the resulting balance between these competing interactions gives the experimentally observed lattice. One may speculate that during growth the C_{60} molecules form a lattice corresponding to the favourable adsorption sites, but that this lattice is unstable and spontaneously dewets, altering the interface and giving the observed epitaxy.

C_{60} on alkali halides undergoes a spontaneous dewetting process resulting in an unusual branched island morphology. This is likely driven by competition between commensurate and coincident lattices similar to that observed for perylene derivatives. Further work characterizing the morphology and evolution during and immediately following deposition to characterize the unstable monolayer would be of interest for understanding the origin and stability of the early-time structures and characterizing this spontaneous dewetting process.

4.3. Pentacene on SiO_2: dewetting in a technologically important system

The thin film growth of pentacene is of considerable technological interest due its use as a prototypical organic semiconductor and its superior performance in thin film FET devices [92–94]. Thin films of pentacene, a planar molecule consisting of a five aromatic rings arranged in a line (see

figure 11(a)), form a herringbone structure much like the bulk crystal with molecules arranged such that they are nearly perpendicular to the surface with only a small tilt angle relative to the surface normal (see figure 11(d)). Typically, pentacene thin films on SiO_2 are well ordered, though polycrystalline. Since the charge transport is believed to occur within the first few molecular layers adjacent to the dielectric interface in OTFTs [4–6], these devices are very often sensitive to interface structure. The use of organic self-assembled monolayers (SAMs) to tune the interface of pentacene OTFTs has been explored [95, 96, 2, 7] and the effect of SAM modification on growth of pentacene thin films has also been examined and discussed in terms of surface energy modification [16].

A recent study of pentacene growth on SiO_2 and Au(111) performed by Käfer *et al* [12] reported evidence of significant post-deposition dewetting on both of these substrates. On SiO_2, layer-by-layer growth is initially observed with the first monolayer nearly completed before subsequent layer formation, followed by substantial roughening. XPS measurements of the C 1s peak and the Si 2p were used to monitor the area covered by pentacene islands (island base area) versus the area of the exposed SiO_2 substrate, respectively. This was done during growth, during annealing, and post-deposition. Deposition at low temperatures (200 K) resulted in homogeneous pentacene films which were then annealed and monitored for changes in the proportion of the surface which was covered by pentacene (the island base area). No significant rapid change was observed until ∼325 K. Interestingly, at similar temperatures, a significant change in the pentacene island morphology measured by AFM was also observed, changing from pyramidal islands to block-like dendritic islands. The authors note that since a phase transition occurs in this same range from the 'thin film' phase to the more tilted bulk phase that this morphological change may be accompanied by a crystallographic rearrangement of the pentacene molecules in the film [12].

Of particular note, is the evolution of the pentacene film after deposition even at temperatures below this annealing transition. The XPS signals here again correspond to a reduction in the area covered by pentacene occurring over the course of some 10s of minutes following deposition (see figure 10). Since desorption can be excluded by thermally programmed desorption (TPD) data, this again must be attributed to a substantial rearrangement of the film. The intensity versus time curves were empirically fit to a sigmoidal Weibull function, representing a smooth exponential transition from one state to the other, and permitting a quantitative characterization of the timescale involved in the dewetting dynamics much as in the case of PTCDI on NaCl. With increased temperature, the pentacene film exhibits the same process occurring on a faster timescale, indicating a thermally activated process. Film thickness was also shown to play a role, with thicker films evolving more slowly due to the larger amount of material involved in this rearrangement. It should be noted that similar dynamics were observed for pentacene on Au(111), although in that case the first monolayer is chemisorbed and remains post-dewetting. No strongly adsorbed monolayer was observed from the TPD spectra taken for pentacene on SiO_2 [12].

The temporal evolution and thermally induced changes of these pentacene films raise potential questions about thermal and long-term stability of thin film pentacene devices on SiO_2, as well as other similar systems. This highlights the importance of tracking device characteristics over relevant timescales and exploring temperature tolerances of organic thin films for technological applications. Additionally, exploration of films during and immediately prior to growth can give insight into how to better control the final film morphology, especially where dewetting is concerned.

The structure of vacuum deposited pentacene thin films on SiO_2 has also been examined in order to better understand and improve device characteristics [6, 97]. A recent study by Mannsfeld *et al* utilizing grazing incidence x-ray diffraction (GIXD) has addressed the structure in great detail [6] (see article for experimental details and structure refinement methods). Of particular interest in this study, is the determination of a monolayer structure which differs from the 'thin film' phase. While both exhibit the herringbone lattice which is similar to the bulk crystal structure, the pentacene molecules of the first monolayer was found to stand exactly perpendicular to the SiO_2 substrate with an *a*–*b* unit cell that is significantly smaller than either the thin film phase or the bulk crystal. As the thickness of the film is increased, the thin film phase is observed with a tilt angle that is ∼5°–6° with respect to the surface normal and lattice constants that are more similar to the bulk pentacene crystal.

Also of particular relevance for organic thin film devices, calculations indicated that the transport through this monolayer structure differs from the 'thin film' tilted phase. Due to the change in symmetry between the edge–face interactions, charge transport should be improved for this configuration [6]. This emphasizes the importance of understanding the detailed structure of molecular films at the dielectric interface as small changes in the structure may influence device-related properties.

It may be that the monolayer phase of pentacene wets the surface, due to a stronger molecule–substrate interaction, but is not compatible with thicker film growth much like the case of PTCDA on NaCl and KCl. Given sufficient energy and/or time, this film may reconstruct to the thin film phase, or if given further energy ($T > 340$ K) even the bulk phase resulting in a different morphology. There are still open questions remaining regarding the stability and structure of this technologically important system, and additional characterization of the interface structure and dynamics both during and *after* growth are required as well as detailed modelling which can capture the potentially important changes at the molecular scale in conjunction with large scale morphological rearrangements.

Modification of gate dielectric surfaces through the use of self-assembled monolayers (SAMs) is sometimes used in organic electronics to tune dielectric properties, surface energy, interface structure, or a combination thereof (see for example [95, 96, 2, 7]). A recent investigation by Amassian *et al* [16] investigates growth and post-deposition behaviour of pentacene thin films on SiO_2, hexamethyldisilazane (HDMS) modified SiO_2, and fluorinated octyltrichlorosilane (FOTS) modified SiO_2 using *in situ* time resolved x-ray reflectivity

(TR-XRR) and *ex situ* AFM. TR-XRR measurements during growth indicate similar progression of the film structure on all three surfaces, with a nearly complete first layer in all cases, and subsequent roughening of the film. AFM measurements show significant post-deposition dewetting of thin films of pentacene on the SAM modified substrates. In these cases, the AFM data shows the initiation of holes or pits adjacent to islands, indicating growth of islands through mass transport from the interface layer in a situation similar to that observed for PTCDA on NaCl [22]. While in this study no dewetting was observed for pentacene on bare SiO_2, contrary to the results described above, subtle differences between experimental conditions, including deposition method, may influence the formation and structure of the interface layer which is expected to dictate the occurrence of dewetting. Rearrangement of the films was also not observed for coverages of more than ∼5 ML, indicating that any re-organization necessary has already occurred during growth, or that the buried interface becomes trapped and can no longer rearrange. Interestingly, re-organization was also not observed for films on HDMS and FOTS modified SiO_2 which were exposed to an ambient environment, indicating that this exposure to air may passivate hole nucleation sites and stabilize the films. However, since exposure to air is generally considered detrimental to the performance of organic thin film devices, the evolution of these films in inert environments remains of substantial importance.

4.4. Overview of example systems

In the examples described here there are two main commonalities: a morphological transition occurs which is accompanied by, and most likely driven by, a change in the interface structure. The dewetting transitions observed for perylene derivatives on alkali halides provide the most striking example of this with an apparent change in epitaxy for several of these systems from commensurate layer(s) to islands with bulk-like lattice parameters [22, 23] much like the simple 1D example illustrated in figure 2. However, as seen in the case of PTCDA on KBr, when near lattice matching occurs between the molecular overlayer and substrate, dewetting is not observed despite similar bulk surface energies. Comparing the measured experimental lattice observed after dewetting to the 'ideal' adsorption lattice determined from calculated minimum energy adsorption sites, a similar effect may also occur for C_{60} on alkali halides. Lastly, while it remains somewhat unclear for pentacene on SiO_2 as the detailed structure and observation of dewetting have not appeared in a single unified study, the dewetting transition observed for this system may arise from the different structure observed for monolayer pentacene which has both a different tilt angle and lattice constants than either the 'thin film' or bulk phases [6].

The formation of metastable films with lattices differing from the anticipated bulk molecular crystals gives rise to the thickness dependant interactions, which are prerequisite for dewetting. In cases where the surface energies of the deposit and substrate are similar, the growth mode will be primarily dictated by the interface energy and these thickness dependent interactions making these systems particularly likely to undergo dewetting as appears to be the case for many molecule on insulator systems. In these situations, examination of lattice mismatch, or the molecular arrangements of thin film structures may provide a predictor of whether or not dewetting will occur.

Lastly, it should be noted that in two of the systems discussed, branched structures are formed as a result of dewetting. The thick branches which occur for PTCDA on NaCl form as a result of the haphazard addition of material from nearby dewetting monolayer islands [73]. C_{60} on alkali halides exhibits very unique branched structures, which are remarkably stable once formed [21]. These shapes may arise from the amplification of fluctuations during the spontaneous dewetting process in the so-called 'spinodal' regime. In both cases, the equilibrium shapes formed through either annealing or high substrate temperature depositions, differ significantly, indicating that films which undergo dewetting may have very different morphology as a result of this process.

5. Summary

The process of dewetting is well known for liquids and polymers, whereby a film is broken up and transformed into droplets or crystallites. Recent studies indicate that this applies also to organic crystalline films deposited in vacuum, and may even be relatively common. The thickness dependent free energy, also termed the disjoining pressure, is a requisite for dewetting and arises from a combination of long range molecule–substrate forces and structuring of the crystalline film, and are specific to the system under consideration as these ultrathin films are often of molecular dimension. The examples described here exhibit dewetting due to a change in the molecule–substrate interface structure, specifically an alteration of the epitaxial relation and/or a change in the molecular orientation at the interface. The occurrence of dewetting in organic films appears to be particularly prevalent on insulating, or otherwise low surface energy, surfaces due to a close competition of the surface energies of the two bulk materials, as well as a close competition between adsorption and intermolecular interactions. Since many organic materials have low surface energies, including polymer materials, this may also have consequences for organic thin films on 'plastics'. Additionally, the compliance of organic materials further accommodates substrate induced strains leading to the easy formation of multiple epitaxies. These readily formed different interface structures can give rise to thickness dependent interaction providing the conditions for dewetting.

Further study of dewetting molecular systems where the details of the interface structure as well as the film evolution during growth and post-deposition re-organization of films are all known will continue to increase our understanding of the driving forces and necessary conditions for dewetting. The development of a predictive framework through the analysis of such experiments and detailed modelling from the molecular scale to the large scale film morphology will further our understanding of stability and morphology of organic films. Theoretical treatment of these systems, spanning the molecular scale to relevant film morphology scales, characterizing the

energetic conditions which predispose dewetting of organic films and the dependence of the stability on molecular scale processes is needed. Calculation of the disjoining pressure for some of these 'prototypical' dewetting systems would be of interest to elucidate the key parameters which drive and control dewetting. Experimentally, molecular mobility (diffusion) may be altered by varying the substrate temperature, which changes the rate of dewetting as well as the final island size. The appearance of post-deposition temporal evolution data, like that highlighted in the examples here, should help to provide a basis for theory, however more studies like these carefully quantifying dewetting dynamics and stability are needed. This will allow for the engineering of higher quality organic thin films and may serve to increase the performance of future organic thin film devices. Furthermore, investigation of how dewetting is influenced by substrate structures may lead to new methods for creating controlled nanostructured deposits of molecular materials, similar to that shown for gold on structured Si/SiO_2 [74]. This approach may apply particularly well to insulating surfaces which can be structured by a number of means [98] and where nanoscale pits on alkali halides have already been shown to template the growth of molecules [63, 64, 26]. Methods of *tuning* film morphology and the rate of dewetting through total coverage, surface templating and temperature control are currently under investigation. Preliminary results for PTCDI on NaCl indicate that the resultant island density, size, and rate of dewetting may be tuned by templating the substrate with single atomic depth pits, depositing gold nanoclusters, or a combination of the two to modify nucleation. The characterization of parameters and conditions which stabilize metastable films or interface structures will be of great importance so that novel properties of films of this nature can be utilized in technological applications.

Acknowledgments

The authors would like to thank Wei Ji and Hong Guo, Quonyong Wang, Dan Vernon and Martin Grant, and Aram Amassian for providing advance copies of manuscripts in process. The authors would also like to thank Jeffrey Mativetsky, Shawn Fostner, Jeffrey LeDue, Roland Bennewitz and Jorge Viñals for discussions. The following funding agencies are gratefully acknowledged for their support: NSERC, CFI, FQRNT, CIfAR, CMP and RQMP.

References

[1] Forrest S R 1997 Ultrathin organic films grown by organic molecular beam deposition and related techniques *Chem. Rev.* **97** 1793–896
[2] Liu S H, Wang W C M, Briseno A L, Mannsfeld S C E and Bao Z N 2009 Controlled deposition of crystalline organic semiconductors for field-effect-transistor applications *Adv. Mater.* **21** 1217–32
[3] Forrest S R 2004 The path to ubiquitous and low-cost organic electronic appliances on plastic *Nature* **428** 911–8
[4] Dimitrakopoulos C D and Malenfant P R L 2002 Organic thin film transistors for large area electronics *Adv. Mater.* **14** 99
[5] Karl N 2003 Charge carrier transport in organic semiconductors *Synth. Met.* **133/134** 649–57
[6] Mannsfeld S C B, Virkar A, Reese C, Toney M F and Bao Z 2009 Precise structure of pentacene monolayers on amorphous silicon oxide and relation to charge transport *Adv. Mater.* **21** 2294
[7] Braga D and Horowitz G 2009 High-performance organic field-effect transistors *Adv. Mater.* **21** 1473–86
[8] Witte G and Woll C 2004 Growth of aromatic molecules on solid substrates for applications in organic electronics *J. Mater. Res.* **19** 1889–916
[9] Schreiber F 2004 Organic molecular beam deposition: growth studies beyond the first monolayer *Phys. Status Solidi* a **201** 1037–54
[10] Beernink G, Strunskus T, Witte G and Woll C 2004 Importance of dewetting in organic molecular-beam deposition: pentacene on gold *Appl. Phys. Lett.* **85** 398–400
[11] Kafer D, Ruppel L and Witte G 2007 Growth of pentacene on clean and modified gold surfaces *Phys. Rev.* B **75** 085309
[12] Kafer D, Woll C and Witte G 2009 Thermally activated dewetting of organic thin films: the case of pentacene on SiO_2 and gold *Appl. Phys.* A **95** 273–84
[13] Krause B, Durr A C, Schreiber F, Dosch H and Seeck O H 2003 Thermal stability and partial dewetting of crystalline organic thin films: 3,4,9,10-perylenetetracarboxylic dianhydride on Ag(111) *J. Chem. Phys.* **119** 3429–35
[14] Witte G, Hanel K, Sohnchen S and Woll C 2006 Growth and morphology of thin films of aromatic molecules on metals: the case of perylene *Appl. Phys.* A **82** 447–55
[15] Frank P, Koch N, Koini M, Rieger R, Müllen K, Resel R and Winkler A 2009 Layer growth and desorption kinetics of a discoid molecular acceptor on Au(111) *Chem. Phys. Lett.* **473** 321–5
[16] Amassian A, Pozdin V A, Desai T V, Hong S, Woll A R, Ferguson J D, Brock J D, Malliaras G G and Engstrom J R 2009 Post deposition reorganization of pentacene films deposited on low-energy surfaces *J. Mater. Chem.* **19** 5580–92
[17] Rath S and Port H 2006 Dewetting of thin UHV-deposited organic films *Chem. Phys. Lett.* **421** 152–6
[18] Tang Y H, Wang Y, Wang G, Wang H B, Wang L X and Yan D H 2004 Vacuum-deposited submonolayer thin films of a three-ring bent-core compound *J. Phys. Chem.* B **108** 12921–6
[19] Durr A C, Schreiber F, Ritley K A, Kruppa V, Krug J, Dosch H and Struth B 2003 Rapid roughening in thin film growth of an organic semiconductor (diindenoperylene) *Phys. Rev. Lett.* **90** 016104
[20] Zhang X N, Barrena E, de Oteyza D G and Dosch H 2007 Transition from layer-by-layer to rapid roughening in the growth of DIP on SiO_2 *Surf. Sci.* **601** 2420–5
[21] Burke S A, Mativetsky J M, Fostner S and Grutter P 2007 C_{60} on alkali halides: epitaxy and morphology studied by noncontact AFM *Phys. Rev.* B **76** 035419
[22] Burke S A, Ji W, Mativetsky J M, Topple J M, Fostner S, Gao H-J, Guo H and Grutter P 2008 Strain induced dewetting of a molecular system: bimodal growth of PTCDA on NaCl *Phys. Rev. Lett.* **100** 186104
[23] Dienel T, Loppacher C, Mannsfeld S C B, Forker R and Fritz T 2008 Growth-mode-induced narrowing of optical spectra of an organic adlayer *Adv. Mater.* **20** 959
[24] Topple J M, Burke S A, Fostner S and Grutter P 2009 Thin film evolution: dewetting dynamics of a bimodal molecular system *Phys. Rev.* B **79** 205414
[25] Fendrich M, Lange M, Weiss C, Kunstmann T and Moller R 2009 N,n'-dimethylperylene-3,4,9,10-bis (dicarboximide) on alkali halide (001) surfaces *J. Appl. Phys.* **105** 094311
[26] Burke S A, LeDue J M, Topple J M, Fostner S and Grutter P 2009 Organic semiconductors: relating the functional properties of an organic semiconductor to molecular structure by nc-AFM *Adv. Mater.* **21** 2029–33

[27] Venables J A 2000 *Introduction to Surface and Thin Film Processes* (Cambridge: Cambridge University Press)
[28] Zangwill A 1988 *Physics at Surfaces* (Cambridge: Cambridge University Press)
[29] Israelachvili J 1991 *Intermolecular and Surface Forces* 2nd edn (London: Academic)
[30] deGennes P-G, Brochard-Wyart F and Quéré D 2004 *Capillarity and Wetting Phenomena: Drops, Bubbles, Pearls, Waves* (New York: Springer)
[31] deGennes P G 1985 Wetting—statics and dynamics *Rev. Mod. Phys.* **57** 827–63
[32] Thiele U 2003 Open questions and promising new fields in dewetting *Eur. Phys. J.* E **12** 409–16
[33] Kim H I, Mate C M, Hannibal K A and Perry S S 1999 How disjoining pressure drives the dewetting of a polymer film on a silicon surface *Phys. Rev. Lett.* **82** 3496–9
[34] Reiter G 1993 Unstable thin polymer-films—rupture and dewetting processes *Langmuir* **9** 1344–51
[35] Bonn D, Eggers J, Indekeu J, Meunier J and Rolley E 2009 Wetting and spreading *Rev. Mod. Phys.* **81** 739–805
[36] Thurmer K, Williams E D and Reutt-Robey J E 2003 Dewetting dynamics of ultrathin silver films on Si(111) *Phys. Rev.* B **68** 155423
[37] Derjaguin B V and Churaev N V 1974 Structural component of disjoining pressure *J. Colloid Interface Sci.* **49** 249–55
[38] Mitlin V S 1993 Dewetting of solid-surface—analogy with spinodal decomposition *J. Colloid Interface Sci.* **156** 491–7
[39] Hooks D E, Fritz T and Ward M D 2001 Epitaxy and molecular organization on solid substrates *Adv. Mater.* **13** 227
[40] Koch S W, Rudge W E and Abraham F F 1984 The commensurate incommensurate transition of krypton on graphite—a study via computer-simulation *Surf. Sci.* **145** 329–44
[41] Kowarik S, Gerlach A and Schreiber F 2008 Organic molecular beam deposition: fundamentals, growth dynamics, and *in situ* studies *J. Phys.: Condens. Matter* **20** 184005
[42] Stohr M, Gabriel M and Moller R 2002 Investigation of the growth of PTCDA on Cu(110): an STM study *Surf. Sci.* **507** 330–4
[43] Ji W, Lu Z-Y and Gao H 2006 Electron core–hole interaction and its induced ionic structural relaxation in molecular systems under x-ray irradiation *Phys. Rev. Lett.* **97** 246101
[44] Ji W, Lu Z-Y and Gao H-J 2008 Multichannel interaction mechanism in a molecule–metal interface *Phys. Rev.* B **77** 113406–4
[45] Ji W, Burke S A, Gao H-J, Grütter P and Guo H 2009 Electronic hybridization of molecules on insulating surfaces submitted
[46] Girifalco L A 1992 Molecular properties of C_{60} in the gas and solid phases *J. Phys. Chem.* **96** 858–61
[47] Northrup J E, Tiago M L and Louie S G 2002 Surface energetics and growth of pentacene *Phys. Rev.* B **66** 121404(R)
[48] Vanzeggeren F and Benson G C 1957 Calculation of the surface energies of alkali halide crystals *J. Chem. Phys.* **26** 1077–82
[49] Knieling T, Lang W and Benecke W 2007 Gas phase hydrophobisation of MEMS silicon structures with self-assembling monolayers for avoiding in-use sticking *Sensors Actuators* B **126** 13–7
[50] Kawai A and Kawakami J 2003 Characterization of SiO_2 surface treated by HMDS vapor and O_2 plasma with AFM tip *J. Photopolym. Sci. Technol.* **16** 665–8
[51] Tyson W R and Miller W A 1977 Surface free-energies of solid metals—estimation from liquid surface-tension measurements *Surf. Sci.* **62** 267–76
[52] Da Silva J L F, Stampfl C and Scheffler M 2006 Converged properties of clean metal surfaces by all-electron first-principles calculations *Surf. Sci.* **600** 703–15
[53] Glockler K, Seidel C, Soukopp A, Sokolowski M, Umbach E, Bohringer M, Berndt R and Schneider W D 1998 Highly ordered structures and submolecular scanning tunnelling microscopy contrast of PTCDA and DM-PBDCI monolayers on Ag(111) and Ag(110) *Surf. Sci.* **405** 1–20
[54] Grobis M, Lu X and Crommie M F 2002 Local electronic properties of a molecular monolayer: C_{60} on Ag(001) *Phys. Rev.* B **66** 161408
[55] Lu X H, Grobis M, Khoo K H, Louie S G and Crommie M F 2003 Spatially mapping the spectral density of a single C_{60} molecule *Phys. Rev. Lett.* **90** 096802
[56] Swarbrick J C, Ma J, Theobald J A, Oxtoby N S, O'Shea J N, Champness N R and Beton P H 2005 Square, hexagonal, and row phases of PTCDA and PTCDI on Ag-Si(111)root 3× root 3r30 degrees *J. Phys. Chem.* B **109** 12167–74
[57] Swarbrick J C, Rogers B L, Champness N R and Beton P H 2006 Hydrogen-bonded PTCDA-melamine networks and mixed phases *J. Phys. Chem.* B **110** 6110–4
[58] Rosei F, Schunack M, Naitoh Y, Jiang P, Gourdon A, Laegsgaard E, Stensgaard I, Joachim C and Besenbacher F 2003 Properties of large organic molecules on metal surfaces *Prog. Surf. Sci.* **71** 95–146
[59] Pradhan N A, Liu N and Ho W 2005 Vibronic spectroscopy of single C_{60} molecules and monolayers with the STM *J. Phys. Chem.* B **109** 8513
[60] Repp J, Meyer G, Paavilainen S, Olsson F E and Persson M 2006 Imaging bond formation between a gold atom and pentacene on an insulating surface *Science* **312** 1196–9
[61] Yamada H, Fukuma T, Umeda K, Kobayashi K and Matsushige K 2002 Local structures and electrical properties of organic molecular films investigated by non-contact atomic force microscopy *Appl. Surf. Sci.* **188** 391–8
[62] Burke S A, Mativetsky J M, Hoffmann R and Grutter P 2005 Nucleation and submonolayer growth of C_{60} on KBr *Phys. Rev. Lett.* **94** 096102
[63] Nony L, Gnecco E, Baratoff A, Alkauskas A, Bennewitz R, Pfeiffer O, Maier S, Wetzel A, Meyer E and Gerber C 2004 Observation of individual molecules trapped on a nanostructured insulator *Nano Lett.* **4** 2185–9
[64] Mativetsky J M, Burke S A, Fostner S and Grutter P 2007 Templated growth of 3,4,9,10-perylenetetracarboxylic dianhydride molecules on a nanostructured insulator *Nanotechnology* **18** 105303
[65] Maier S, Fendt L A, Zimmerli L, Glatzel T, Pfeiffer O F, Diederich F and Meyer E 2008 Nanoscale engineering of molecular porphyrin wires on insulating surfaces *Small* **4** 1115–8
[66] Albrecht T R, Grutter P, Horne D and Rugar D 1991 Frequency-modulation detection using high-Q cantilevers for enhanced force microscope sensitivity *J. Appl. Phys.* **69** 668–73
[67] Wagner T, Bannani A, Bobisch C, Karacuban H, Stohr M, Gabriel M and Moller R 2004 Growth of 3,4,9,10-perylenetetracarboxylic-dianhydride crystallites on noble metal surfaces *Org. Electron.* **5** 35–43
[68] Gustafsson J B, Zhang H M and Johansson L S O 2007 STM studies of thin PTCDA films on Ag/Si(111)-$\sqrt{3} \times \sqrt{3}$ *Phys. Rev.* B **75** 155414
[69] Schlettwein D, Back A, Schilling B, Fritz T and Armstrong N R 1998 Ultrathin films of perylenedianhydride and perylenebis(dicarboximide) dyes on (001) alkali halide surfaces *Chem. Mater.* **10** 601–12
[70] Seidel C, Awater C, Liu X D, Ellerbrake R and Fuchs H 1997 A combined STM, LEED and molecular modelling study of PTCDA grown on Ag(110) *Surf. Sci.* **371** 123–30
[71] Ogawa T, Kuwamoto K, Isoda S, Kobayashi T and Karl N 1999 3,4:9,10-perylenetetracarboxylic dianhydride (PTCDA) by electron crystallography *Acta Crystallogr.* B **55** 123–30
[72] Silly F and Castell M R 2006 Bimodal growth of Au on $SrTiO_3$ (001) *Phys. Rev. Lett.* **96** 086104
[73] Burke S A 2009 Building foundations for molecular electronics: growth of organic molecules on alkali halides as prototypical insulating substrates *PhD Thesis* McGill University, Montreal, Canada Can be retrieved through http://digitool.library.mcgill.ca:8881/R/
[74] Giermann A L and Thompson C V 2005 Solid-state dewetting for ordered arrays of crystallographically oriented metal particles *Appl. Phys. Lett.* **86** 121903

[75] Kunstmann T, Schlarb A, Fendrich M, Wagner T, Moller R and Hoffmann R 2005 Dynamic force microscopy study of 3,4,9,10-perylenetetracarboxylic dianhydride on KBr(001) *Phys. Rev.* B **71** 121403(R)
[76] Tojo K and Mizugushi J 2002 Refinement of the crystal structure of 3,4:9,10-perylene-bis(dicarboximide), $C_{24}H_{10}N_2O_4$, at 263 K *Z. Kristallogr.* **217** 45 (Data deposited at the Cambridge Crystallographic Data center (CCDC) File: LENPEZ01, No. CCDC 187633)
[77] Guillermet O, Mossoyan-Deneux M, Giorgi M, Glachant A and Mossoyan J C 2006 Structural study of vapour phase deposited 3,4,9,10-perylene tetracarboxylicacid diimide: comparison between single crystal and ultra thin films grown on Pt(100) *Thin Solid Films* **514** 25–32
[78] Harris L A and Clancy P 2006 A 'partitioned leaping' approach for multiscale modeling of chemical reaction dynamics *J. Chem. Phys.* **125** 144107
[79] Choudhary D, Clancy P, Shetty R and Escobedo F 2006 A computational study of the sub-monolayer growth of pentacene *Adv. Funct. Mater.* **16** 1768–75
[80] Luthi R, Haefke H, Meyer E, Howald L, Lang H P, Gerth G and Guntherodt H J 1994 Frictional and atomic-scale study of C_{60} thin-films by scanning force microscopy *Z. Phys.* B **95** 1–3
[81] Cavar E, Blum M C, Pivetta M, Patthey F, Chergui M and Schneider W D 2005 Fluorescence and phosphorescence from individual C-60 molecules excited by local electron tunneling *Phys. Rev. Lett.* **95** 196102
[82] Joachim C and Gimzewski J K 1997 An electromechanical amplifier using a single molecule *Chem. Phys. Lett.* **265** 353–7
[83] Dresselhaus M S, Dresselhaus G and Eklund P C 1993 Fullerenes *J. Mater. Res.* **8** 2054–97
[84] Segura J L, Martin N and Guldi D M 2005 Materials for organic solar cells: the C_{60}/pi-conjugated oligomer approach *Chem. Soc. Rev.* **34** 31–47
[85] Tanigaki K, Kuroshima S and Ebbesen T W 1995 Crystal-growth and structure of fullerene thin-films *Thin Solid Films* **257** 154–65
[86] Yase K, Ara-Kato N, Hanada T, Takiguchi H, Yoshida Y, Back G, Abe K and Tanigaki N 1998 Aggregation mechanism in fullerene thin films on several substrates *Thin Solid Films* **331** 131–40
[87] Kim Y, Jiang L, Iyoda T, Hashimoto K and Fujishima A 1998 AFM study of surface phenomena based on C_{60} film growth *Appl. Surf. Sci.* **130** 602–9
[88] Zhang Z Y and Lagally M G 1997 Atomistic processes in the early stages of thin-film growth *Science* **276** 377–83
[89] Wang Q, Vernon D and Grant M, Multilayer surface growth and physisorption on insulating substrate submitted, private communication
[90] Ji W, private communication
[91] Jung S C and Kang M H 2008 First-principles study of a single C_{60} cluster adsorbed on KBr(100) *Surf. Sci.* **602** 1916–20
[92] Shtein M, Mapel J, Benziger J B and Forrest S R 2002 Effects of film morphology and gate dielectric surface preparation on the electrical characteristics of organic-vapor-phase-deposited pentacene thin-film transistors *Appl. Phys. Lett.* **81** 268–70
[93] Klauk H, Halik M, Zschieschang U, Schmid G, Radlik W and Weber W 2002 High-mobility polymer gate dielectric pentacene thin film transistors *J. Appl. Phys.* **92** 5259–63
[94] Reese C, Chung W J, Ling M M, Roberts M and Bao Z N 2006 High-performance microscale single-crystal transistors by lithography on an elastomer dielectric *Appl. Phys. Lett.* **89** 202108
[95] McDowell M, Hill I G, McDermott J E, Bernasek S L and Schwartz J 2006 Improved organic thin-film transistor performance using novel self-assembled monolayers *Appl. Phys. Lett.* **88** 073505
[96] Hill I G, Weinert C M, Kreplak L and van Zyl B P 2009 Influence of self-assembled monolayer chain length on modified gate dielectric pentacene thin-film transistors *Appl. Phys.* A **95** 81–7
[97] Schiefer S, Huth M, Dobrinevski A and Nickel B 2007 Determination of the crystal structure of substrate-induced pentacene polymorphs in fiber structured thin films *J. Am. Chem. Soc.* **129** 10316
[98] Bennewitz R 2006 Structured surfaces of wide band gap insulators as templates for overgrowth of adsorbates *J. Phys.: Condens. Matter* **18** R417–35